Structural Engineering and Mechanics, *Vol. 73, No. 4 (2020) 437-445*
DOI: https://doi.org/10.12989/sem.2020.73.4.437

Local bond–slip behavior of fiber reinforced LWAC after exposure to elevated temperatures

Chao-Wei Tang*[1,2,3]

[1]*Department of Civil Engineering & Geomatics, Cheng Shiu University, No. 840, Chengching Rd., Niaosong District, Kaohsiung City, Taiwan R.O.C.*
[2]*Center for Environmental Toxin and Emerging-Contaminant Research, Cheng Shiu University, No. 840, Chengching Rd., Niaosong District, Kaohsiung 83347, Taiwan*
[3]*Super Micro Mass Research & Technology Center, Cheng Shiu University, No. 840, Chengching Rd., Niaosong District, Kaohsiung 83347, Taiwan*

(Received January 22, 2019, Revised October 9, 2019, Accepted October 15, 2019)

Abstract. The microstructure and mechanical properties of concrete will degrade significantly at high temperatures, thus affecting the bond strength between reinforcing steel and surrounding concrete in reinforced concrete members. In this study, the effect of individual and hybrid fiber on the local bond–slip behavior of lightweight aggregate concrete (LWAC) after exposure to elevated temperatures was experimentally investigated. Tests were conducted on local pullout specimens (150 mm cubes) with a reinforcing bar embedded in the center section. The embedment lengths of the pullout specimens were 4.2 times the bar diameter. The parameters investigated included concrete type (control group: ordinary LWAC; experimental group: fiber reinforced LWAC), concrete strength, fiber type, and targeted temperature. The test results showed that for medium-strength LWACs exposed to high temperatures, the use of only steel fibers did not significantly increase the residual bond strength. Moreover, the addition of individual and hybrid fiber had little effect on the residual bond strength of the high-strength LWAC after exposure to a temperature of 800°C.

Keywords: fiber reinforced lightweight aggregate concrete, residual bond strength, pullout test

1. Introduction

Lightweight aggregate (LWA) with a smaller unit weight or specific gravity can be used to replace ordinary aggregate to produce lightweight aggregate concrete (LWAC) (Somayaji 2001). The use of LWAC can reduce structural weight by more than 20%, and thus effectively decreasing the seismic loads on building structures (Chandra and Berntsson 2002, Tang 2015, Tang 2017). It also can reduce the installation and transportation costs of pre-cast members. However, LWAC exhibits higher brittleness and lower mechanical properties than normal weight concrete (NWC) of the same compressive strength (Gao *et al*. 1997, Hassanpour *et al*. 2012). Studies have shown that the use of fibers in LWAC is a suitable solution to resolve such problems (Ding and Kusterle 2000, Li 2002, Mehta and Monteiro 2006).

According to the nature of fiber, it may be classified into the metallic fiber, inorganic fiber, and organic fiber. Fibers of various shapes and sizes made of steel, plastic, glass, and natural materials are often used in concrete (Metha and Monteiro 2006). Incorporation of fibers will affect the fresh and mechanical properties of concrete, depending on the type and percentage of fiber (ACI Committee 544 1982, Nematzadeh and Poorhosein 2017). In general, the incorporation of fibers in LWAC, as single or hybrid forms, can improve its mechanical properties, and significantly increase its toughness, ductility performance, and energy absorption, while decreasing its workability, particularly when steel fiber is used in LWAC mixture (Campione *et al*. 2005, Kurugol *et al*. 2008, Hassanpour *et al*. 2012).

In reinforced concrete (RC) structures, the bond strength between reinforcing steel and surrounding concrete plays a crucial role, which is the essential element for concrete and steel to work together as a kind of composite material (ACI Committee 408 2003). The effect of rebar diameter, rebar embedded length in concrete, concrete strength and type, cover thickness, and crack spacing on the bond strength between rebar and concrete has been extensively investigated. (Hossain 2008, Alexandre *et al*. 2014, Deng *et al*. 2014, Golafshani *et al*. 2014, Dehestani and Mousavi 2015, Mo *et al*. 2015, Choi and Lee 2015, Kim *et al*. 2016, Lee and Yi 2016, Xu *et al*. 2016, Zhang and Yu 2016, Al-Shannag and Charif 2017, Bilek *et al*. 2017, Saleem 2017, Ahmad *et al*. 2018, Tang 2018). Overall, their test results indicated that the load-slip behavior of the deformed steel bars embedded in concrete was mainly dependent on concrete compressive strength, diameter of rebar, and length of rebar embedment. Moreover, the lower particle strength in LWAC resulted in lower bond splitting strengths and reduced post-elastic straining as compared to NWC. Therefore, ACI 318-14 recommended some correction factors to reflect the lower tensile strength of LWAC, which can reduce shear strength, friction properties, splitting

*Corresponding author, Ph.D., Professor
E-mail: tangcw@gcloud.csu.edu.tw

ISSN: 1225-4568 (Print), 1598-6217 (Online)

resistance, bond between concrete and reinforcement, and increase development length, compared with NWC of the same compressive strength. (ACI 318-14 2014).

Personal safety in the event of a fire is one of the important considerations in residential, public, and industrial building design. Once the firing temperature reaches the critical concrete temperature of 500°C, the structural performance of RC structures will be seriously degraded (Newman and Choo 2003). In essence, a concrete behavior is the result of many simultaneous interactions when exposed to high temperatures. Generally, the high temperature will cause the dimensional change of concrete, which is the sum of the changes in the volume of cement paste and aggregate (Metha and Monteiro 2006). In particular, the bond performance in RC structures under elevated temperatures will gradually decrease owing to incompatible dimensional changes between cement paste and aggregate. Moreover, high strength concrete (HSC) in an environment with a rapid increase in temperature is more likely to lead to explosive spalling that is caused by thermal stress due to temperature gradient during heating (Ko *et al*. 2011). This has greatly compromised the structural integrity of RC structures. Therefore, the spalling behavior of HSC subjected to elevated temperatures has attracted many researchers' interest (Xiong and Richard Liew 2015). The literature shows that polypropylene fibers can mitigate or prevent explosive spalling (Poon *et al*. 2004, Ding *et al*. 2012, Ozawa and Morimoto 2014, Yan *et al*. 2015). This is mainly due to the fact that polypropylene fibers melt after the temperature inside concrete reaches approximately 170°C, which produces micro channels for the release of the vapor pressure in concrete (Bilodeau *et al*. 2004, Kodur 2014, Xiong and Richard Liew 2015).

In view of the above considerations, the microstructure and mechanical properties of concrete under elevated temperatures may significantly deteriorate and thus affect the bond performance in RC structures. The review of the literature indicates that little research has been undertaken to investigate the role of fibers in maintaining the post-heating bond between LWAC and steel rebar. Further study of the bond behavior of LWC after high temperatures should contribute to the enhancement of existing code provisions for LWAC. Therefore, this study aimed at investigating the local bond–slip behavior of various fiber-reinforced LWACs after exposure to elevated temperatures.

2. Experimental procedure

2.1 Experimental program

The experimental investigation was designed to study the effect of individual and hybrid fiber on the local bond–slip behavior of LWAC after exposure to elevated temperatures. Local pullout tests with a concentric reinforcing bar in concrete were adopted for experimental determination of the local bond-slip relationship between rebar and concrete. The test parameters analyzed included concrete type, concrete strength, fiber type, and targeted temperature. The variables for the test are shown in Table l.

Table 1 Planning of experimental variables

Group	Mix No.	Specified concrete strength	Fiber content (Volume %)	Targeted temperature (°C)
Control group	C30	30 MPa	0	400, 600, and 800
	C50	50 MPa	0	400, 600, and 800
Experimental group	E30-S	30 MPa	Steel fiber (1%)	400, 600, and 800
	E50-S	50 MPa	Steel fiber (1%)	400, 600, and 800
	E50-P	50 MPa	Polypropylene fiber (0.1%)	400, 600, and 800
	E50-M	50 MPa	Steel fiber (1%) + Polypropylene fiber (0.1%)	400, 600, and 800

Table 2 Physical properties of fine aggregate

Aggregate type	Specific weight (SSD)	Water absorption (SSD) (%)	FM
Fine aggregate	2.60	1.25	2.70

Notes: SSD=saturated surface dry condition; FM=fineness modulus.

Table 3 Physical and mechanical of LWA

Dry specific weight	1-hr Water absorption (%)	Unit weight (dry-rodded) (kg/m^3)	Crushing strength (MPa)
1.2	4.9	707.5	3.6

Table 4 Physical and mechanical of deformed bar

Bar No.	Nominal dia. (mm)	Nominal cross section area (cm^2)	Rib distance (mm)	Rib width (mm)	Rib height (mm)	Yield strength (N/mm^2)
3	9.53	0.71	6.1	3.4	0.5	468.3
6	19.12	2.87	12.3	4.5	1.5	489.5

Table 5 Mix proportions of LWAC

Group	Mix No.	W/B	Cement (kg/m^3)	Slag (kg/m^3)	Water (kg/m^3)	Aggregate (kg/m^3)		SP (kg/m^3)	Steel fiber (kg/m^3)	PP (kg/m^3)
						FA	CA			
Control group	C30	0.50	315	105	210	824	418	2.9	-	-
	C50	0.32	412	138	176	957	348	7.7	-	-
Experimental group	E30-S	0.50	315	105	210	824	418	2.9	78	-
	E50-S	0.32	412	138	176	957	348	7.7	78	-
	E50-P	0.32	412	138	176	957	348	7.7	-	0.9
	E50-M	0.32	412	138	176	957	348	7.7	78	0.9

Note: C=ordinary LWAC; E=fiber reinforced LWAC; digits=strength level; W/B=water/binder ratio; FA=fine aggregate; CA=lightweight coarse aggregate; SP=superplasticizer; PP=polypropylene fiber.

As can be seen from Table 1, the specimens were divided into two groups to investigate the effect of different fibers on their residual bond strength and bond strength-slip response after exposure to elevated temperatures (400, 600, and 800°C).

2.2 Materials

The materials used in this study included cement, slag, fine and coarse aggregates, fiber, superplasticizer, and reinforcing bar. The cement used was local Portland cement with a specific gravity of 3.15 and a fineness of 3400 cm2/g, complying with ASTM C150/C150M (ASTM C150/C150M-15 2015). Local slag with a specific gravity

of 2.9 and a fineness of 6000 cm2/g was used. The fine aggregate was a natural river, complying with ASTM C33/C33M (ASTM C33/C33M-13 2013). The physical properties of the fine aggregate are shown in Table 2. The coarse LWA used was locally produced from reservoir sludge. Its physical and mechanical properties are listed in Table 3. Local steel fibers and polypropylene fibers were used. Sikament-1250 produced by Sika Taiwan Ltd. was used as a superplasticizer in the production of concrete. The reinforcing bars used included No. 3 and No. 6, and their physical and mechanical properties are shown in Table 4.

2.3 Mix proportions

In this study, two types of concrete were prepared: ordinary LWAC and fiber reinforced LWAC, the former serving as the reference concrete. To analyze the influence of concrete strength on the bond behavior, the specified 28-day compressive strengths were chosen equal to 30 and 50 MPa for medium- and high-strength concrete, respectively. Some trial mixtures were prepared to obtain the target strength at 28 days, along with proper workability of 150 to 220 mm. The mix proportions of the control group and the experimental group are given in Table 5. The abbreviations for identifying each concrete indicate the type of concrete – control group (C) or experimental group (E), the strength of concrete (30 or 50 MPa), and the type of fiber (S: steel fiber, P: polypropylene fiber, M: hybrid fiber).

Before mixing, the aggregates were cured indoors until the required saturated surface-dry condition was reached. In the mixing process, the cement, slag, fiber, fine aggregates, and lightweight coarse aggregates were generally blended first, and then water and superplasticizer were added. The mixing operation was continued until a uniform and homogeneous concrete without any segregation was obtained.

2.4 Casting of specimens

The pullout specimens were cubes of 150 mm with a single No. 6 bar embedded vertically along the central axis (see Fig. 1). As can be seen in Fig. 1, the steel bar was embedded in the center of concrete with 300 mm of the bar length projecting out on one end and 20 mm of the bar on the other end. The embedment length (la) of the bar in the pullout specimens was 4.2 times the bar diameter (d_b), i.e., l_a=4.2d_b. This embedment length is short enough to assume that the bond stresses can be evenly distributed throughout the loading process. In other words, the recorded data can properly represent the local bond stress value (Soroushian *et al*. 1994). Those unbounded regions of the bar were sheathed with a PVC pipe. In addition, three lateral stirrups (No. 3 rebars) were embedded in the test specimens to prevent the concrete from splitting when the longitudinal reinforcing bar was in tension. For each concrete mixture, two nominally identical specimens were tested to check the validity of the test setup and the variations in test results.

The pullout specimens were cast in steel molds. For each mixture, freshly mixed concrete was slowly poured into the pullout specimen mold and then was completely compacted with an external vibrator. In addition, for each mixture, enough cylinder specimens of concrete (100 mm in diameter and 200 mm in height), referred to hereafter as control cylinders, were also cast and compacted with an external vibrator. After casting, the specimens were immediately covered with a wet hessian and polyethylene sheets. The pullout specimens with their respective control cylinders were demolded after 24 hours. Following demolding, the specimens were immediately cured in a standard curing room, until testing at the age of 28 days.

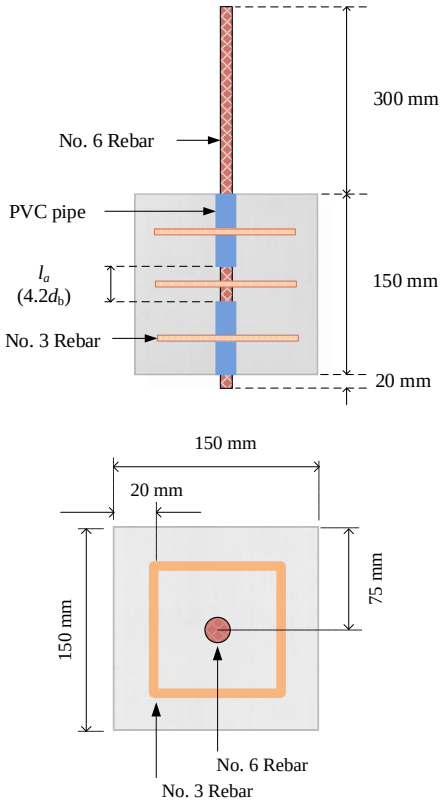

Fig. 1 Dimensions and cross-sections of the test specimen

2.5 Instrumentation and test procedures

Compressive strength test for the concrete cylinders was carried out in accordance with the ASTM C39 standard. Pullout test was performed in accordance with the ASTM C234 standard. An MTS servo controlled universal testing machine was used. The loading machine was capable of applying 500 kN of force in uniaxial tension and also allowed displacement-controlled tests. A detailed outline of the pullout test setup is shown in Fig. 2.

As can be seen in Fig. 2, the test setup comprised of an assembly on which the pullout specimen could be mounted, which was able to effectively measure the relative slippage between rebar and concrete. Linear variable differential transformers (LVDTs) were used to measure the relative bond slip between rebar and concrete at the loaded as well as the free ends. Both ends of the specimen were fixed to the bracket of the displacement device and the 6 mm-LVDTs were installed. Then, the specimen was placed between the two steel plates and the tail end of the rebar was fixed to the punch of the universal testing machine.

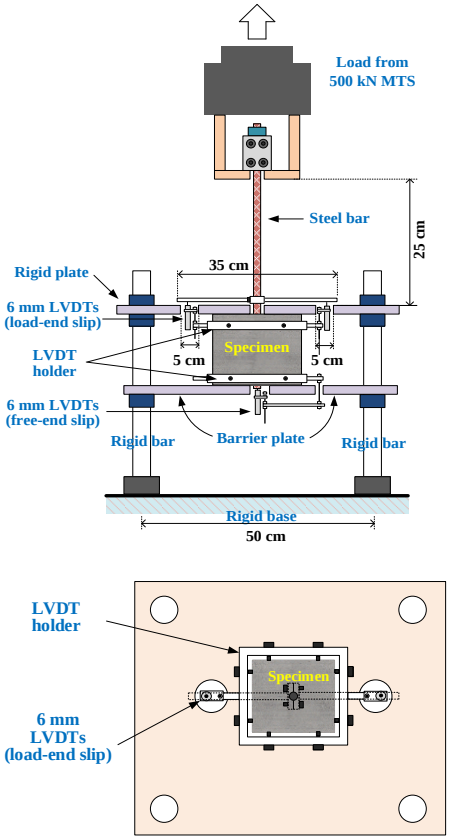

Fig. 2 Schematic for details of the pullout test setup

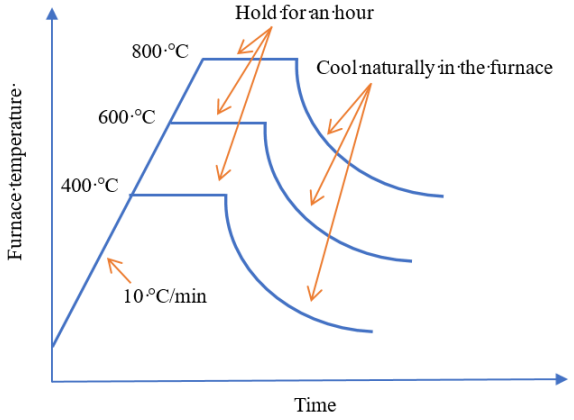

Fig. 3 Temperature versus time curve in the furnace for the pullout specimens

Table 6 Results of the slump, unit weight and compressive test of LWAC

Group	Mix No.	Slump (cm)	Unit weight (kg/m^3)	Compressive strength (MPa)
Control group	C30	20	1875	33.1
	C50	21	2039	58.2
Experimental group	E30-S	18	1953	32.4
	E50-S	18	2117	51.4
	E50-P	20	2040	52.4
	E50-M	16	2118	50.8

Subsequently, a pullout force was applied at a constant displacement rate of 0.01 mm/sec up to bond failure. The pullout force was measured by a load cell fitted in the loading machine. The test progress was monitored on a computer screen, and the load of the machine versus slip relationship was captured and stored on a diskette via a data logger until failure of the specimen.

To investigate the effect of individual and hybrid fiber on the local bond–slip behavior of LWAC after exposure to elevated temperatures, the pullout specimens were heated without preload at a prescribed rate (10°C/min.) until the temperature inside the furnace reached the target temperatures. Once the target maximum temperature had been reached, the furnace temperature was maintained for another hour to achieve a thermal steady state in the whole specimen (Fig. 3). Then, the furnace power switch was turned off, and the specimens were allowed to cool slowly in the furnace at laboratory temperature. The post-fire pullout tests were carried out after the cooling period.

3. Experimental results and discussion

3.1 Fresh and mechanical properties of concrete

Following the mixing procedure, fresh concrete properties were measured immediately. The results of the slump and the unit weight test of concrete in the control and experimental groups are shown in Table 6. As can be seen from Table 6, the slump value ranged from 16 to 21 cm. For the control group, the C30 mix had a slump of 20 cm, and the C50 mix had a slump of 21 cm. These results indicated that the mixtures of the control group had very good workability. As for the experimental group, the E30-S and E50-S mixes with steel fiber had a slump of 18 cm, the E50-P mix with polypropylene fiber had a slump of 20 cm, but the slump of the E50-M mix with steel fiber and polypropylene fiber was only 16 cm. The reason is that the amount of fiber used in the E50-M mix was higher, resulting in a stiffer mixture and leading to reduced workability. In addition, for medium-strength LWAC, the unit weights were 1875 and 1953 kg/m^3 for the C30 and E30-S mixes, respectively. In other words, there was no significant difference in unit weight between the two mixes. For high strength LWAC, the unit weight of the C50, E50-S, E50-P, and E50-M mixes with the addition of fiber was ranged from 2039 to 2118 kg/m^3, which can meet the requirements of LWAC.

At 28 days of age, the cylinders of each mix were capped with gypsum capping compound and tested in compression to determine the compressive strength of concrete. A mean value of concrete compressive strength was calculated by taking an average of three specimens. As can be seen from Table 6, the compressive strength of the control group and the experimental group was higher than the 28-day design compressive strength at room temperature. In addition, comparing the strength of concrete

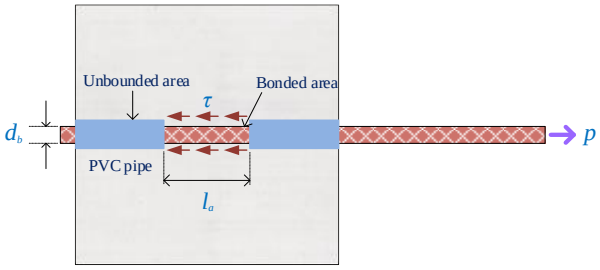

Fig. 4 Schematic diagram of local bond stress between bar and concrete

with medium-strength (the C30 and E30-S mixes), it can be seen that the addition of steel fiber did not increase the compressive strength of concrete at 28 days of age. For high strength concrete, the compressive strengths of the experimental group (the E50-S, E50-P, and E50-M mixes) were also lower than that of the control group (the C50 mix).

3.2 Local bond stress–slip relationship

During the pullout test, by measuring the relative slip between concrete and rebar, the local bond stress versus slip curve of the specimen can be obtained. Assuming that the bond stress is uniformly distributed along the bonded length (see Fig. 4), the bond stress can be obtained from the internal force balance condition of the specimen. Therefore, the measured bond strength was calculated using Eq. (1) given below:

$$\tau = \frac{P}{\pi d_b l_a} \tag{1}$$

where τ is the bond stress (MPa); P is the pullout force (N); d_b is the bar diameter (mm); l_a is the bond length (mm).

Basically, the relative slip between steel bar and concrete corresponding to the bond stress can be divided into the loading end slip s_l and the free end slip s_f. In the case of a local bond, the relative slip of the steel and concrete can be idealized as rigid body motion. In other words, the s_l and s_f should be the same under the same loading. Therefore, the average of the two is the slip of the corresponding bond stress, as follows:

$$s = \frac{s_l + s_f}{2} \tag{2}$$

The local bond stress and slip can be calculated using Eq. (1) and Eq. (2), respectively. The local bond stress versus slip curves at different temperatures for the medium- and high-strength LWAC specimens are shown in Fig. 5 and Fig. 6, respectively. Overall, the pullout specimens were a shear failure. In other words, the concrete between the steel ribs was sheared off and the rebar slipped in a frictional mode of failure. At room temperature, the behavior of the bond stress-slip relationship of the specimens was characterized by an initial increase in the bond stress with negligible slips due to the adhesion between rebar and matrix. However, as the load increased, the adhesion gradually declined. When the load increased continuously

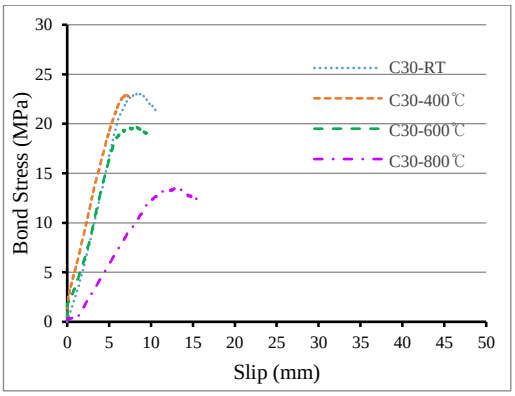

(a) Control group

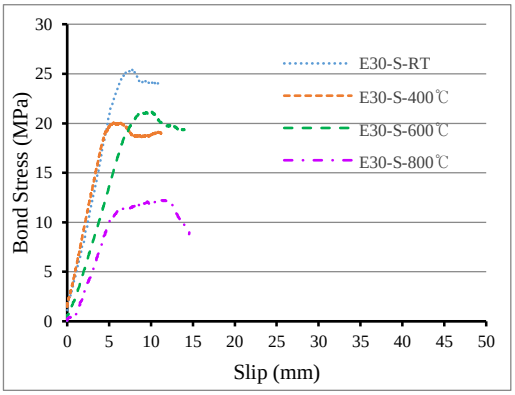

(b) Experimental group

Fig. 5 Local bond stress versus slip curve of medium-strength LWAC

and the bond stress reached splitting bond stress (τ_{cr}), radial splits appeared around the rebar due to radial pressure exerted by the wedging action of the lugs of the rebar. After that, there was a relative slip between the rebar and the matrix, and once the ultimate bond stress (τ_u) had been reached, softening occurs. Almost immediately thereafter, the bond stress decreased quickly and the slip increased sharply. Eventually, when the amount of slip reached one to two times the net spacing of the ribs, only the friction between the rebar and the surrounding concrete can be considered as the residual bond stress (τ_f).

For the medium-strength LWAC, the relationship between bond stress and slip is shown in Fig. 5. As can be seen from Fig. 5, at room temperature, the ultimate bond stress of the control group (the C30 mix) and the experimental group (the E30-S mix) demonstrated similar responses up to the peak value, but different energy dissipation in the post-peak branch. Overall, the incorporation of steel fibers could enhance the post-peak branch of the local bond stress versus slip curve. In addition, the ultimate bond stress of the C30 specimen was only slightly attenuated after exposure to 400°C, but the ultimate bond stress of the E30-S specimen was obviously attenuated.

As for the high strength LWAC, the local bond stress-slip curves are shown in Fig. 6. It is worth mentioning that, with the increase of concrete strength, the splitting bond stress (τ_{cr}) in the local bond stress versus slip curve of the

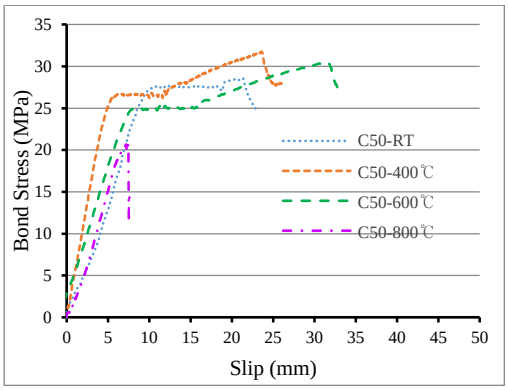

(a) Control group C50

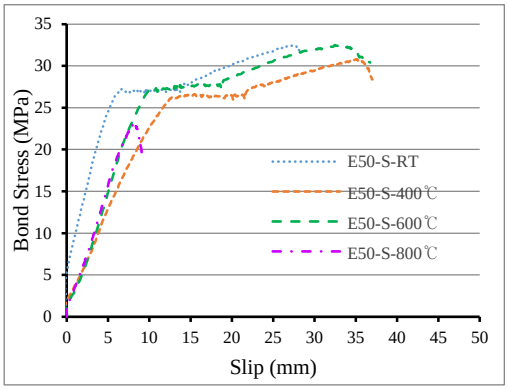

(b) Experimental group E50-S

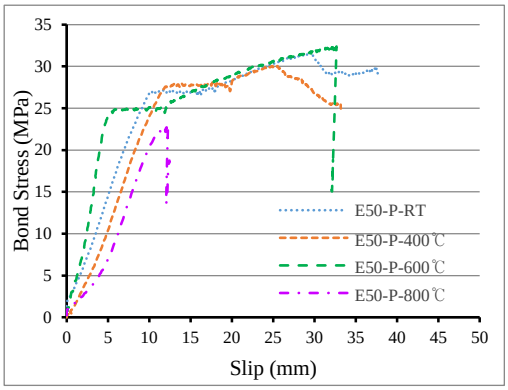

(c) Experimental group E50-P

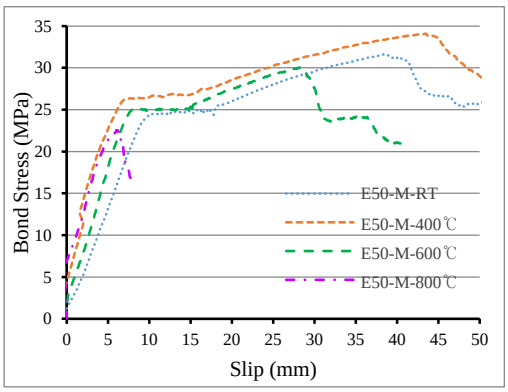

(d) Experimental group E50-M

Fig. 6 Local bond stress versus slip curve of high-strength LWAC

Table 7 Results of bond stress, residual bond stress, and residual bond strength ratio

Group	Mix No.	Bond strength (MPa)	Residual bond strength (MPa)			Residual bond strength ratio		
		Room temperature	Exposure temperature (°C)			Exposure temperature(°C)		
			400	600	800	400	600	800
Control group	C30	22.9	22.8	19.7	13.5	1.00	0.86	0.59
	C50	28.6	31.5	30.3	20.6	1.10	1.06	0.72
Experimental group	E30-S	25.5	20.6	21.1	12.2	0.81	0.83	0.48
	E50-S	32.5	30.5	32.2	23.1	0.94	0.99	0.71
	E50-P	31.6	30.0	32.1	22.7	0.95	1.02	0.72
	E50-M	31.6	34.0	30.7	22.6	1.08	0.97	0.72

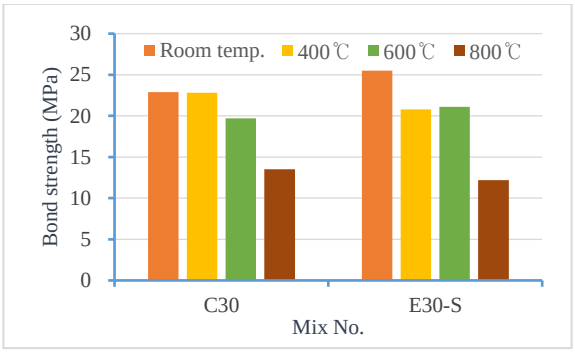

(a) Medium-strength LWAC

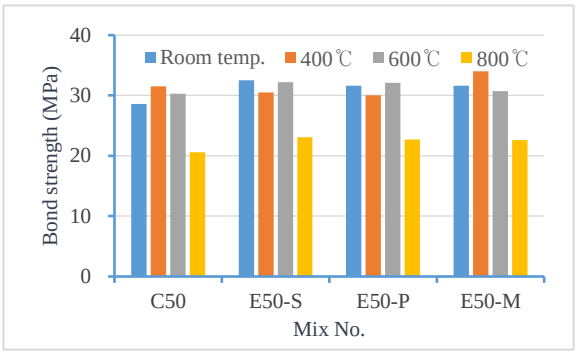

(b) High-strength LWAC

Fig. 7 Comparison of bond strength for LWAC mixes

high strength LWAC was higher than that of the medium-strength LWAC. As can be seen from Fig. 6(a) and Fig. 6(d), the ascending slope of the local bond stress versus slip curve of the C50 mix and E50-M mix specimens significantly increased after exposure to 400-600°C. The reason is mainly due to the drying effect of the specimen at high temperature, resulting in an increase in the strength of the concrete (Siddique and Kaur 2012). In addition, the evaporable water was removed due to the drying effect at a high temperature, and the pore pressure formed by the high temperature can be reduced to increase the ultimate bonding stress. However, Fig. 6(b) and Fig. 6(c) show that the ascending slope of the E50-S and E50-P specimens at different temperatures was more complicated. On the other hand, after exposure to 800°C, the ultimate bond stress of the control group and the experimental group specimens was significantly attenuated.

3.3 Ultimate bond stress

Table 7 presents the experimental results of ultimate bond stress for all specimens of different concrete mixtures at different temperatures. As can be seen from Table 7, the bond strength at 28 days of age in the control group and the experimental group can be higher than 22 MPa at room temperature. In addition, comparing the bond strength of moderate strength concretes (the C30 and E30-S mixes), it can be concluded that the incorporation of steel fiber did improve its 28-day bond strength. On the other hand, for the 28-day bond strength of the high strength concrete, the value of the experimental group specimens was greater than that of the control group specimen.

Table 7 also lists the residual bond strength of each concrete mixture after being exposed to different high temperatures. In the control group, the residual bond strength of the C30 mix was between 13.5-22.8 MPa, while the residual bond strength of the C50 mix was between 20.6-31.5 MPa. In the experimental group, the residual bond strength ranged from 12.2 to 21.1 MPa, from 23.1 to 32.2 MPa, from 22.7 to 32.1 MPa, and from 22.6 to 34.0 MPa for the E30-S, E50-S, E50-P, and E50-M mixes, respectively.

The residual bond strength of each concrete mixture after being exposed to different high temperatures is compared, as shown in Fig. 7. As can be seen from Table 7, the residual strength ratio of these specimens was about 0.48 to 1.11 after exposure to elevated temperatures. As can be seen from Fig. 7, the residual bond strength of each concrete mixture showed different trends with the increasing temperature. Fig. 8(a) shows that for the medium-strength concrete, after exposure to 400°C, the residual bond strength of the C30 mix maintained the same value without attenuation, while the residual bond strength of the E30-S mix significantly attenuated. Moreover, after exposure to 600°C, the residual bond strength of the C30 mix slightly decayed, whereas the residual bond strength of the E30-S mix slightly increased. However, once the temperature was raised to 800°C, the residual bond strength of the C30 and E30-S mixes significantly decreased, and the residual strength ratios were lower than 0.60. In addition, it can be seen from Fig. 8(b) that the trend of the residual bond strength ratio in the control group and the experimental group was similar to that in Fig. 8(a). From these test results, it can be seen that for medium-strength concrete, the use of steel fibers did not significantly improve the residual bond strength of LWAC.

As for the high-strength concrete, it can be seen from Fig. 9(a) that the residual bond strengths of the specimens were more complicated with the increasing temperature. After exposure to 400-600°C, the residual bond strength of some specimens was higher than that at room temperature. It can be seen from Fig. 9(a) that the residual bond strength of the E50-M mix after exposure to 400°C was the largest. The reason may be due to the increased tensile strength of steel fibers to resist thermal stress. Additionally, when the internal temperature of the concrete reached about 170°C, the polypropylene fibers melted and provided microchannels to reduce the vapor pressure in the concrete. As a result, the E50-M mix can exhibit a better residual

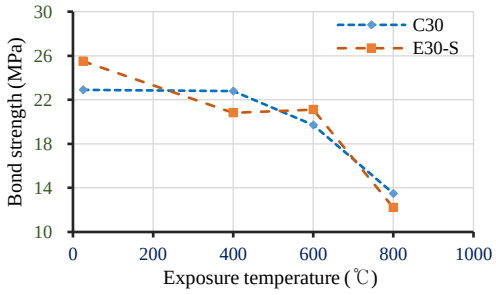

(a) Residual bond strength

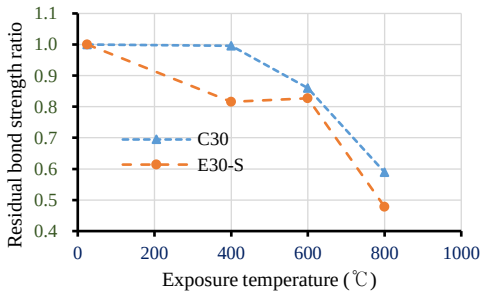

(b) Residual bond strength ratio

Fig. 8 Comparison of bond strength for medium-strength LWAC mixes

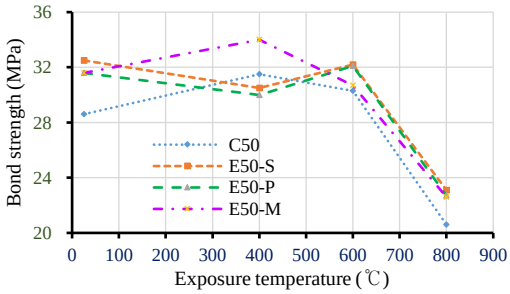

(a) Residual bond strength

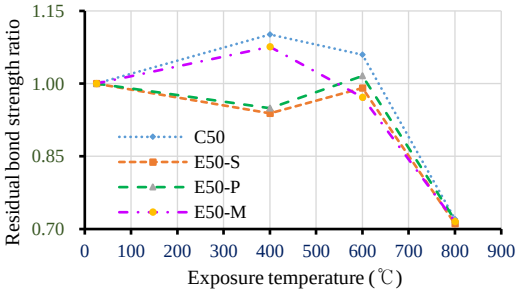

(b) Residual bond strength ratio

Fig. 9 Comparison of bond strength for high strength LWAC mixes

bond strength. In other words, in a hybrid fiber reinforced LWAC, steel fibers can contribute to the residual mechanical properties after heat exposure, while PP fibers reduced explosive spalling. However, the residual bond strength of all specimens decreased significantly after exposure to 800°C. As can be seen from Fig. 9(b), when the temperature was over 600°C, there was not much different in terms of the residual bond strength ratio between the

experimental group and the control group. From this perspective, the addition of fiber on the residual bond strength of high-strength concretes after exposure to a temperature of 800°C was not significant.

4. Conclusions

In this study, steel fiber and polypropylene fiber were used to investigate the effects of individual and hybrid fiber on the local bond stress-slip relationship of medium- and high-strength LWAC after exposure to elevated temperatures. Based on the above experimental results and discussion, the following conclusions were drawn:

- With the increase of compressive strength of fiber reinforced LWAC, the ultimate bond stress in the local bond stress-slip curve also increased.
- For medium-strength LWACs exposed to high temperatures, the use of only steel fibers does not significantly increase the residual bond strength. After exposure to 400°C, the residual bond strength of the C30 mix maintained the same value without attenuation, while the residual bond strength of the E30-S mix significantly attenuated. Moreover, after exposure to 600°C, the residual bond strength of the C30 mix slightly decayed, whereas the residual bond strength of the E30-S mix slightly increased. Once the temperature was raised to 800°C, the residual bond strength of the C30 and E30-S mixes significantly decreased, and the residual strength ratios were lower than 0.60.
- For high-strength LWACs, the residual bond strengths of the specimens were more complicated with the increasing temperature. After exposure to 400-600°C, the residual bond strength of some specimens was higher than that at room temperature. After exposure to 400°C, the residual bond strength of the E50-M mix was the largest. This indicated that the steel fibers can contribute to the residual mechanical properties after heat exposure, while PP fibers reduced explosive spalling. However, there was not much different in terms of the residual bond strength ratio between the experimental group and the control group after exposure to 800°C. This indicated that the addition of individual and hybrid fiber had little effect on the residual bond strength of the high-strength LWAC after exposure to a temperature of 800°C.

Acknowledgments

This work was supported by the Ministry of Science and Technology (MOST), Taiwan. The author expresses his gratitude and sincere appreciation to MOST for financing this research work.

References

ACI Committee 544 (1982), "State of the art report of fiber reinforced concrete", *Concr. Int.: Des. Construct.*, **4**(5), 9-30.

ACI Committee 408 (2003), *Bond and Development of Straight Reinforcing Bars in Tension (ACI 408R-03)*, American Concrete Institute, Farmington Hills, Mich., U.S.A.

ACI-318 (2014), *Building Code Requirements for Reinforced Concrete and Commentary*, American Concrete Institute, Farmington Hills, Mich., U.S.A.

Ahmad, S., Pilakoutas, K., Rafi, M.M., Zaman, Q.U. (2018), "Bond strength prediction of steel bars in low strength concrete by using ANN", *Comput. Concrete*, **22**(2), 249-259. https://doi.org/10.12989/cac.2018.22.2.249.

Alexandre Bogas J., Gomes, M.G., Real, S. (2014), "Bonding of steel reinforcement in structural expanded clay lightweight aggregate concrete: The influence of failure mechanism and concrete composition", *Construct. Build Mater.*, **65**, 350-359. https://doi.org/10.1016/j.conbuildmat.2014.04.122.

Al-Shannag, M.J. and Charif, A. (2017), "Bond behavior of steel bars embedded in concretes made with natural lightweight aggregates", *J. King Saud U. Eng. Sci.*, **29**, 365-372. https://doi.org/10.1016/j.jksues.2017.05.002.

ASTM C150/C150M-15 (2015), *Standard Specification for Portland Cement*, ASTM International, West Conshohocken, PA, www.astm.org.

ASTM C33/C33M-13 (2013), *Standard Specification for Concrete Aggregates*, ASTM International, West Conshohocken, PA, www.astm.org.

Bilek, V., Bonczková, S., Hurta, J., Pytlík, D. and Mrovec, M. (2017), "Bond strength between reinforcing steel and different types of concrete", *Procedia Eng.*, **190**, 243-247. https://doi.org/10.1016/j.proeng.2017.05.333.

Bilodeau, A., Kodur, V.K.R. and Hoff, G.C. (2004), "Optimization of the type and amount of polypropylene fibres for preventing the spalling of lightweight concrete subjected to hydrocarbon fire", *Cement Concrete Compos.*, **26**, 163-174. https://doi.org/10.1016/S0958-9465(03)00085-4.

Campione, G., Cucchiara, C., Mendola, L.L. and Papia, M. (2005), "Steel–concrete bond in lightweight fiber reinforced concrete under monotonic and cyclic actions", *Eng Struct*, **27**, 881-890. https://doi.org/10.1016/j.engstruct.2005.01.010.

Chandra, S. and Berntsson, L. (2002), *Lightweight Aggregate Concrete*, Noyes Publications, New York, U.S.A.

Choi, J.I., Lee, B.Y. (2015), "Bonding properties of basalt fiber and strength reduction according to fiber orientation", *Materials*, **8**(10), 6719-6127. https://doi.org/10.3390/ma8105335.

Dehestani, M., MoU.S.Avi, S.S. (2015), "Modified steel bar model incorporating bond-slip effects for embedded element method", *Construct. Build Mater.*, **81**, 284-290. https://doi.org/10.1016/j.conbuildmat.2015.02.027.

Deng, Z.C., Jumbe, R.D., Yuan, C.X. (2014), "Bonding between high strength rebar and reactive powder concrete", *Comput. Concrete*, **13**(3), 411-421. https://doi.org/10.12989/cac.2014.13.3.411.

Ding, Y. and Kusterle, W. (2000), "Compressive stress–strain relationship of steel fibrereinforced concrete at early age", *Cem Concr Res*, **30**, 1573-1579. https://doi.org/10.1016/S0008-8846(00)00348-3.

Ding, Y., Azevedo, C., Aguiar, J.B., Jalali, S. (2012), "Study on residual behaviour and flexural toughness of fibre cocktail reinforced self compacting high performance concrete after exposure to high temperature", *Construct. Build Mater.*, **26**, 21-31. https://doi.org/10.1016/j.conbuildmat.2011.04.058.

Gao, J., Suqa, W. and Morino, K. (1997), "Mechanical properties of steel fiber-reinforced, high-strength, lightweight concrete", *Cem Concr Compos*, **19**, 307-313. https://doi.org/10.1016/S0958-9465(97)00023-1.

Golafshani, E.M., Rahai, A., Kebria, S.S.H. (2014), "Prediction of the bond strength of ribbed steel bars in concrete based on genetic programming", *Computers & Concrete*, **14**(3), 327-359. https://doi.org/10.12989/cac.2014.14.3.327.

Hassanpour, M., Shafigh, P. and Mahmud, H.B. (2012), "Lightweight aggregate concrete fiber reinforcement – A

review", *Construct. Build Mater.*, **37**, 452-461. https://doi.org/10.1016/j.conbuildmat.2012.07.071.

Hossain, K.M.A. (2008), "Bond characteristics of plain and deformed bars in lightweight pumice concrete", *Constr. Build. Mater.*, **22**, 1491-1499. https://doi.org/10.1016/j.conbuildmat.2007.03.025

Kim, N.W., Lee, H.H., Kim, C.H. (2016), "Fracture behavior of hybrid fiber reinforced concrete according to the evaluation of crack resistance and thermal", *Comput. Concrete*, **18**(5), 685-696.

Ko, J., Ryu, D., Noguchi, T. (2011), "The spalling mechanism of high-strength concrete under fire", *Mag. Concr. Res.*, **63**(5), 357-370. http://dx.doi.org/10.1680/macr.10.00002.

Kodur, V. (2014), "Properties of concrete at elevated temperatures", *ISRN Civil Engineering*, 1-15. https://doi.org/10.1155/2014/468510.

Kurugol, S., Tanacan, L. and Ersoy, H.Y. (2008), "Young's modulus of fiber-reinforced and polymer-modified lightweight concrete composites", *Constr Build Mater*, **22**, 1019-1028. https://doi.org/10.1016/j.conbuildmat.2007.03.017.

Lee, H.H., Yi, S.T. (2016), "Structural performance evaluation of steel fiber reinforced concrete beams with recycled aggregates", *Comput. Concrete*, **18**(5), 741-756. https://doi.org/10.4334/JKCI.2015.27.3.215.

Li, V.C. (2002), "Large volume high performance applications of fibers in civil engineering", *J. Appl. Polym. Sci.*, **83**(3), 660-686. https://doi.org/10.1002/app.2263.

Mehta, P.K., Monteiro, P.J.M. (2006), *Concrete: Microstructure, Properties, and Materials*, 3rd edition, The McGraw-Hill Companies, Inc., New York, U.S.A.

Mo, K.H., Alengaram, U.J., Visintin, P., Goh, S.H., Jumaat, M.Z. (2015), "Influence of lightweight aggregate on the bond properties of concrete with various strength grades", *Construct. Build Mater.*, **84**, 377-386. https://doi.org/10.1016/j.conbuildmat.2015.03.040.

Newman, J. and Choo, B.S. (2003), *Advanced Concrete Technology 2: Concrete Properties*, 1st edition., Butterworth-Heinemann, United Kingdom.

Nematzadeh, M., Poorhosein, R. (2017), "Estimating properties of reactive powder concrete containing hybrid fibers using UPV", *Comput. Concrete*, **20**(4), 4915-502. https://doi.org/10.12989/cac.2017.20.4.491.

Ozawa, M., Morimoto, M. (2014), "Effects of various fibres on high-temperature spalling in high-performance concrete", *Construct. Build Mater.*, **71**, 83-92. https://doi.org/10.1016/j.conbuildmat.2014.07.068.

Poon, C.S., Shui, Z.H., Lam, L. (2004), "Compressive behavior of fiber reinforced high-performance concrete subjected to elevated temperatures", *Cement Concrete Res.,* **34**, 2215-2222. https://doi.org/10.1016/j.cemconres.2004.02.011.

Saleem, M. (2017), "Study to detect bond degradation in reinforced concrete beams using ultrasonic pulse velocity test method", *Struct. Eng. Mech.*, **64**(4), 427-436. https://doi.org/10.12989/sem.2017.64.4.427.

Siddique, R. and Kaur, D. (2012), "Properties of concrete containing ground granulated blast furnace slag (GGBFS) at elevated temperatures", *J. Adv. Res.*, **3**, 45-51. https://doi.org/10.1016/j.jare.2011.03.004.

Somayaji, S. (2001), *Civil Engineering Materials*, 3rd edition, Prentice Hall, New Jersey, U.S.A.

Soroushian, P., Mirza, F., Alhozaimy, A. (1994), "Bonding of confined steel fiber reinforced concrete to deformed bars", *ACI Mater. J.*, **91**(2), 144-149.

Tang, C.W. (2015), "Local bond stress-slip behavior of reinforcing bars embedded in lightweight aggregate concrete", *Comput. Concrete*, **16**(3), 449-466. http://dx.doi.org/10.12989/cac.2015.16.3.449.

Tang, C.W. (2017), "Uniaxial bond stress-slip behavior of reinforcing bars embedded in lightweight aggregate concrete", *Struct. Eng. Mech.*, **62**(5), 651-661. https://doi.org/10.12989/sem.2017.62.5.651.

Tang, C.W. (2018), "Local bond-slip behavior of medium and high strength fiber reinforced concrete after exposure to high temperatures", *Struct. Eng. Mech.*, **66**(4), 477-485. https://doi.org/10.12989/sem.2018.66.4.477.

Xiong, M.X., Richard Liew, J.Y. (2015), "Spalling behavior and residual resistance of fibre reinforced Ultra-High performance concrete after exposure to high temperatures", *Materiales de Construccion*, **65**, 320. https://doi.org/10.3989/mc.2015.00715.

Xu, M., Hallinan, B., Wille, K. (2016), "Effect of loading rates on pullout behavior of high strength steel fibers embedded in ultra-high performance concrete", *Cement Concrete Compos.*, **70**, 98-109. https://doi.org/10.1016/j.cemconcomp.2016.03.014.

Yan, Z., Shen, Y., Zhu, H., Li, X., Lu, Y. (2015), "Experimental investigation of reinforced concrete and hybrid fibre reinforced concrete shield tunnel segments subjected to elevated temperature", *Fire Safety J.*, **71**, 86-99. https://doi.org/10.1016/j.firesaf.2014.11.009.

Zhang, H., Yu, R.C. (2016), "Inclined Fiber Pullout from a Cementitious Matrix: A Numerical Study", *Materials*, **9**(10), 800. https://doi.org/10.3390/ma9100800.

CC